Int. J. Heat Mass Transfer. Vol. 35, No. 2, pp. 421–431, 1992
Printed in Great Britain

0017–9310/92 \$5.00+0.00

Freezing of a paraffin flow downstream of an abrupt expansion

T. A. MYRUM and S. THUMMA
Mechanical Engineering Department, Louisiana State University, Baton Rouge, LA 70803, U.S.A.

(*Received* 4 *October* 1990 *and in final form* 25 *February* 1991)

Abstract—Freezing of a paraffin flow downstream of an abrupt expansion was studied experimentally. Results obtained for three different expansion ratios (d/D) at a constant system flow rate ($Re_D \approx 3400$) and a constant inlet Reynolds number ($Re_d \approx 3400$) demonstrated that the 'ice-band' spacing is a function of the freezing parameter (θ) only and can be predicted to within 8% using a correlation developed for water flow in a constant-area duct. The results also showed that the effect of expansion caused freeze-off to occur at higher θ values, with freeze-off occurring for $7.5 < \theta \leqslant 8.5$, $11 < \theta \leqslant 13$, and $13 < \theta \leqslant 16$, respectively, for $d/D = 1.0$ (no expansion), 0.643, and 0.340.

INTRODUCTION

THE FREEZING of internal liquid flows occurs in numerous situations. In many of these, freezing may have undesirable effects. For instance, water mains could become partially or totally blocked, robbing fire fighters of their most essential tool in controlling life or death situations. Also, each year millions of dollars of damage is done to homes because of the freeze-off and subsequent rupture of domestic piping. In many instances, freezing is desirable, such as in casting processes, desalination of water, freezing of foods, etc.

Whether freezing is desirable or undesirable, it is imperative that the basic freezing phenomena and heat transfer characteristics in freezing flows be understood. To meet this end, a number of investigations have been performed to study freezing flows in straight constant-area ducts. Stefan [1] studied the solid growth within a circular tube analytically by assuming finite ambient heat transfer and imposing a known heat flux along the liquid–solid interface. Solutions for the instantaneous and steady-state shape of the liquid–solid interface under laminar conditions were obtained analytically in ref. [2]. Cho and Özisik [3] and Shibani and Özisik [4] analyzed the transient freezing of turbulent flows in circular tubes and the steady-state freezing between parallel plates, respectively, while Sproston [5] used a conformal transform technique to obtain the interfacial shape inside a rectangular duct.

Freezing flows in channels with external convective cooling have been studied analytically for air-cooled tubes [6], for liquid cooled parallel-plate channels [7, 8] and for turbulent flow in convectively cooled tubes [9]. Natural convection effects were studied analytically and experimentally in ref. [10] and experimentally in refs. [11–13].

Good agreement between analytical and experimental results for freezing in the combined hydrodynamic and thermal entrance region was obtained in ref. [14]. For thin steady-state ice layers in turbulent flow, the combined theoretical and experimental study of ref. [15] showed that small temperature nonuniformities in the wall temperature can produce wide variations in pressure drop. This was also observed for laminar flows by ref. [11].

Reference [16] developed a theoretical technique for predicting the conditions under which freeze-off occurs. Upper and lower bounds for the minimum pressure drop required to prevent freeze-off were obtained by respectively including and excluding natural convection. Companion experimental results were found to lie within these bounds. The numerical/analytical treatment of freezing in laminar tube flow by refs. [17, 18] demonstrated that freeze-off is sensitive to the pumping temperature and pumping capability. Hirata [19] found that the increase in the friction factor associated with bends and valves in a piping system promotes freeze-off.

Gilpin [13] was the first to observe the 'ice-band' structure, a profile with a dramatic cyclic variation along the tube length. It was concluded for an initially laminar flow that the 'ice-band' structure resulted from the natural expansion of the flow passage at the exit of the cooled tube. For an initial turbulent flow [20], it was found that the 'ice-band' structure was independent of the exit condition. Both refs. [20, 21] found that for a given working fluid, the 'ice-band' spacing depended only on the inlet-liquid and tube-wall temperatures. Reference [21] obtained an empirical relation for the 'ice-band' spacing in terms of these parameters.

Two types of solid formation for parallel-plate flows were observed by ref. [22]. These were transition type (abrupt transition from a thick to thin solid layer) and smooth type (a relatively thin layer of uniform thickness). Equations were obtained for the prediction of the occurrence of the two types, for the location in

NOMENCLATURE

D	test section diameter (2.00 cm)
d	inlet diameter
L	test section length (47 cm)
m	mass flow rate
P	instantaneous pressure
P_0	initial pressure before freezing
Re_D	test-section Reynolds number, $4m/\pi D\mu$
Re_d	inlet Reynolds number $4m/\pi d\mu$
S	'ice-band' spacing
$T_{freeze}, T_{in}, T_{out}, T_w$	freezing (28.2°C), inlet, outlet, and tube wall temperatures, respectively
V	average velocity in test section before freezing
x	axial coordinate measured from test section inlet.

Greek symbols

θ	freezing parameter, $(T_{freeze}-T_w)/(T_{in}-T_{freeze})$
μ	dynamic viscosity ($\approx 3.8\times10^{-3}$ kg m^{-1} s^{-1}) at $(T_{in}+T_{out})/2$
ρ	density of paraffin (≈ 760 kg m^{-3}) at $(T_{in}+T_{out})/2$.

the duct where the transition between a smooth- and transition-type layer occurs, and for the heat transfer coefficients along the interface.

Thomason and Mulligan [23] studied the transient pressure drop behavior for a freezing flow. The pressure drop characteristics were found to be quite sensitive to slight changes in the coolant temperature, inlet liquid temperature, and the flow rate. For a particular combination of these parameters, the pressure drop was observed to oscillate periodically for several hours.

All of the preceding investigations concern the freezing in constant-area straight ducts. However, actual piping systems consist of area changes, valves, and bends, and as mentioned earlier, Hirata [19] found that the friction induced by these can promote freezing. To date no work has been performed to assess the effects of bends or sudden area changes (valves or expansions) on freezing.

The purpose of the present experimental investigation was to assess the effect of a sudden channel expansion on the instantaneous shape of the flow passage during freezing downstream of the expansion and the associated instantaneous pressure behavior. Information about the effect of the expansion on freeze-off was also obtained. Experiments were performed for parametric variations of the expansion ratio, flow rate, and the freezing parameter, $\theta = (T_{freeze}-T_w)/(T_{in}-T_{freeze})$, where, respectively, T_{freeze}, T_{in}, and T_w are the freezing temperature (28.2°C), inlet liquid temperature, and tube wall temperature. Ninety-nine percent pure n-octadecane paraffin ($Pr \approx 13$) was the working fluid.

EXPERIMENTAL APPARATUS

As just mentioned 99% n-octadecane paraffin was the working fluid. It was confirmed in ref. [24] and in a set of preliminary experiments during this investigation that n-octadecane exhibits a sharp freezing (melting) point. The fluid was selected because the relatively high freezing temperature reduced the cooling requirements, enabling the use of water as the coolant. In addition, since the freezing point was above room temperature, no extraneous melting occurred during the extraction of the frozen samples from the test section or during the examination of the samples.

Figure 1 shows the key features of the experimental apparatus. First, it is noted that the test section is vertically oriented. This orientation minimizes secondary natural convection effects. Gilpin [13] observed for Reynolds numbers between 370 and 3025 that changing the orientation from horizontal to vertical virtually eliminated natural convection effects.

A gear pump was used to circulate the paraffin around the flow loop. Measurements showed that the maximum decrease in the flow rate due to the flow blockage (no freeze-off) was 6%. However, for most of the experiments, the change in the flow rate was less than 3%. The flow rate was varied by varying the rotational speed of the pump. This was accomplished using a variable-speed d.c. motor. The motor could be controlled to within 2% of its maximum rotational speed, giving a maximum uncertainty, at the lowest rotational speed, of 6.5%.

The most important feature of the flow loop is the test section (see Fig. 1(b)), which is a 2.00 cm i.d., 47 cm long copper tube with a 1.1 mm wall thickness. Five pairs of 0.08 mm diameter, Teflon-coated chromel–constantan thermocouples were evenly distributed over the length of the test section, with the first and last pairs located 1.25 cm from the inlet and outlet of the test section, respectively. The respective members of each pair were positioned diametrically opposite to one another, and each thermocouple junction was 0.25 mm from the inner surface of the tube. Copper oxide cement ($k \approx 2.6$ W m^{-1} °C^{-1}) was used to fix the thermocouple junctions to the tube.

The cooling water, passed through the annular space formed by the outer tube wall and the inner surface of a 4.06 cm i.d. PVC pipe, served to set the wall temperature. The wall temperature was obtained from the arithmetic average of the eight thermo-

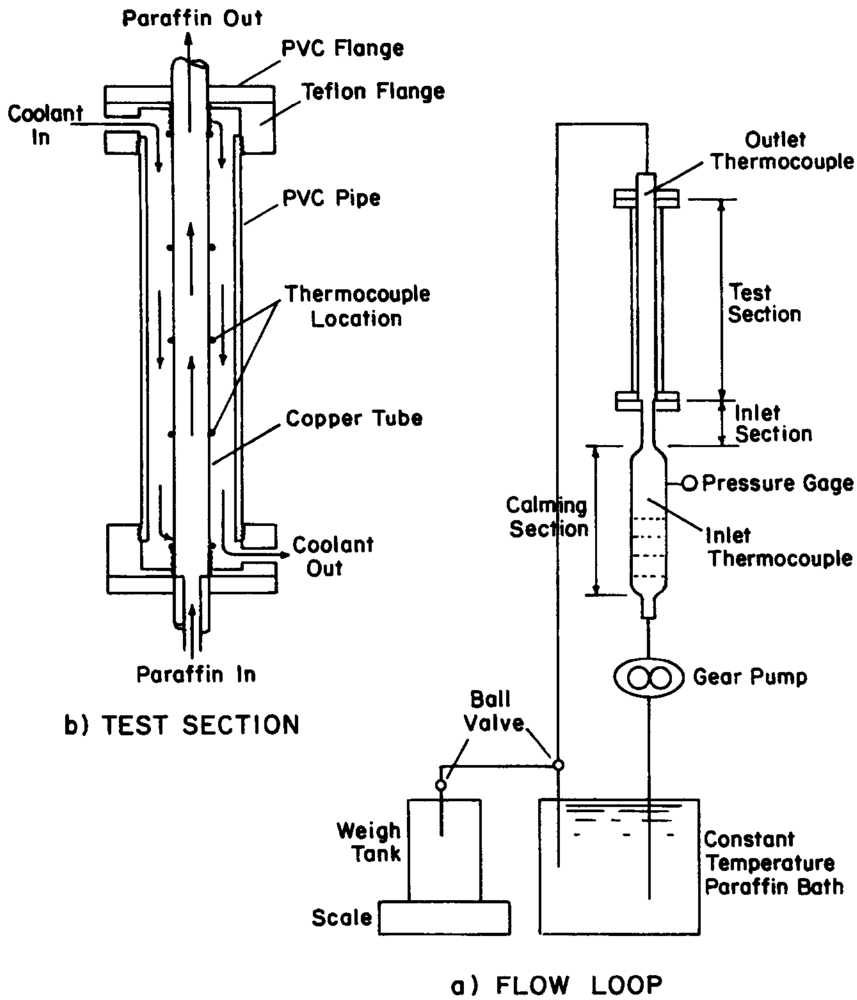

FIG. 1. Experimental apparatus.

couples, with the standard deviation being within $\pm 0.4°C$.

Three different inlet sections were positioned between the calming section and test section, respectively, giving inlet-to-test-section diameter (or expansion) ratios of $d/D = 0.340$, 0.643, and 1.00.

Pressure measurements were performed 15 cm upstream of the entrance to the inlet section using a pressure gage with a resolution of 0.7 kPa and an accuracy of ± 0.2 kPa. This location was one calming chamber diameter (3.7 test-section diameters) downstream of the final calming grid in the chamber and 1.2 calming chamber diameters upstream of the entrance to the tapered exit portion of the chamber.

The inlet temperature was measured at 2.54 cm upstream of the pressure measurement location, while the outlet temperature was measured at the exit plane of the test section. These thermocouples were identical to those used for the test-section wall. All of the thermocouple voltages were read to within ± 5 μV ($\pm 0.08°C$) using a data logger.

EXPERIMENTAL PROCEDURE

Experiments were performed to assess the effect of the expansion ratio (i.e. the inlet-to-test-section diameter ratio) on the instantaneous shape of the flow passage and the associated instantaneous pressure behavior and to assess the effect of the expansion ratio on the value of the freezing parameter, θ, which resulted in complete freeze-off. In the former, the flow rate was varied and θ was fixed, while in the latter, the flow rate was fixed and θ was varied.

Both types of experiments required the same preparatory steps. First, the temperature in the paraffin bath was set to the desired level, as was the temperature of the cooling water. Then, to melt away the residual paraffin left on the walls of the flow loop from the preceding run, the paraffin was circulated at the maximum flow rate for 2 h. Next, the pump speed corresponding to the desired flow rate was set, and the resulting flow rate was measured by diverting the flow into the weigh tank. With the flow measurement complete, the water flow and the data logger were started simultaneously.

For the experiments performed to ascertain the instantaneous flow passage shape, several data runs were performed for a given flow rate, θ value, and expansion ratio, with each data run being characterized by a preselected time interval. At the end of the prescribed time interval, the paraffin and cooling water flows were terminated simultaneously. To prevent extraneous freezing, the test section was cleared of excess paraffin by reversing the flow direction immediately after the termination of the data run. The test section was then removed and the frozen sample was extracted. Subsequently, the solid was sectioned along its length, and the inner diameter of each cross-section was measured to within 0.15 mm using a precision caliper. The measured values were plotted and joined together with a smooth curve to give the instantaneous flow passage shape.

The procedure used to ascertain the critical freeze-off θ value will be discussed at a more appropriate time.

EFFECT OF d/D ON THE FLOW PASSAGE SHAPE

Figures 2–4 display the timewise evolution of flow passage shape for $\theta = 5.4$, $Re_d \approx 3400$ (i.e. the same inlet Reynolds number), and $d/D = 1.0$, 0.643, and 0.340, respectively. The maximum uncertainty in these figures due to the measurement of the flow passage is 6%. The uncertainty in θ is $\pm 4\%$. Figure 2 displays the classical 'ice-band' structure observed by refs. [13, 20–22]. At 5 min (300 s), the flow passage has a slight uniform taper up to about 23 tube diameters, at which point a sudden expansion is observed. The expansion is the result of the flow exiting the cooled test section. With increasing time, the expansion point moves upstream. At about 2 h (7200 s), a second expansion point forms, and it too moves upstream as time passes. After 8 h (28 800 s), the expansion points stop migrating upstream, and the solid profile stops changing, signalling the attainment of a steady-state profile. The fact that steady state was achieved was verified by performing a 20 h run and verifying that the solid had the same shape.

The just described behavior is identical to that observed by ref. [20]. In this work, it was concluded that two criteria are necessary for the development of the 'ice-band' structure. First, the tapered solid layer is unstable to large disturbances, which in this case are supplied by the expansion at the exit. The second requirement is the upstream movement caused by the high heat transfer downstream of the expansion which eats away at the downstream face. It can be seen that melting does occur downstream of the expansion point owing to the turbulence generated as the flow moves through the expansion. As the expansion point moves upstream, the melted region downstream of the expansion also moves upstream. Note the turbulence associated with the flow through the expansion tends to reduce the flow restriction.

Hirata and Ishihara [21] obtained a correlation equation ($S/D = 7.5/\theta^{1.5} - 4.5$) for the steady-state 'ice-band' spacing for water flows. However, the fact that the 'ice-band' spacing is a function of θ only suggested the use of this correlation for the paraffin results of the present study. The 'ice-band' spacing at steady state for the present study is 7.6% greater than that predicted by ref. [21], which is well within the scatter of the experimental data about the curve calculated from the correlation. This finding suggests

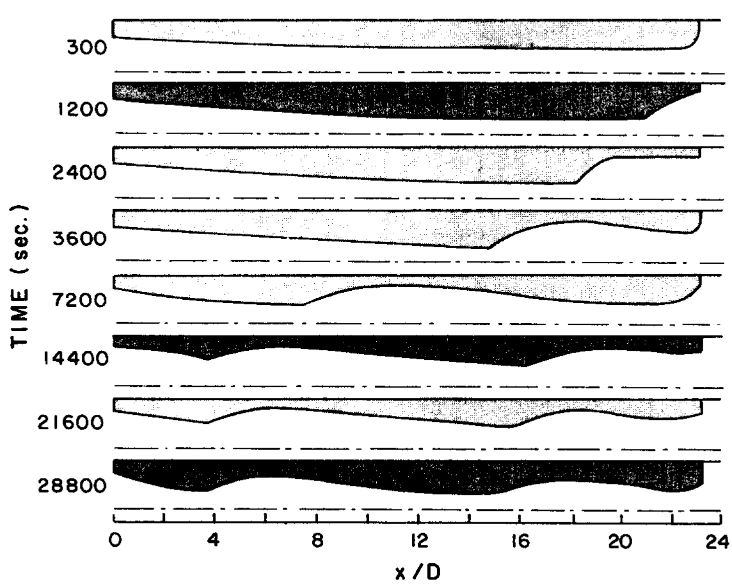

FIG. 2. Instantaneous solid profiles: $d/D = 1.0$, $Re_d = 3410$, $\theta = 5.4$.

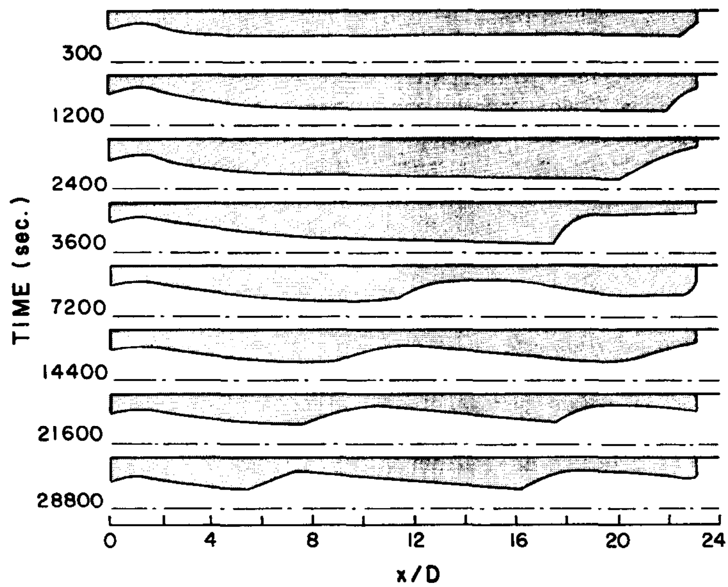

FIG. 3. Instantaneous solid profiles: $d/D = 0.643$, $Re_d = 3450$, $\theta = 5.4$.

that the correlation of ref. [21] can be extended to other fluids.

In contrast to the slowly tapering flow passage observed for all times near the entrance of the test section for $d/D = 1.0$, Fig. 3 shows, for $d/D = 0.643$, the presence of a diverging/converging section between 0 and 2.5 diameters. After about 2.5 diameters, the evolutions of the flow passages for the two cases are rather similar. However, the steady-state position of the upstream expansion point is shifted by 1.8 diameters downstream of that for $d/D = 1.0$, while the downstream point is shifted downstream by about 1.1 diameters. Consequently, the 'ice-band' spacing is 0.7 diameters (or 6%) shorter for $d/D = 0.643$, which is within maximum experimental uncertainty. In addition, the spacing is only 1% greater than that predicted by ref. [21].

Regarding the behavior at the entrance to the test section, the diverging/converging shape can be directly linked to the behavior of the local heat transfer coefficient downstream of an abrupt expansion. References [25, 26] demonstrated that the heat transfer coefficient increases in the downstream direction in the separated region until it attains its

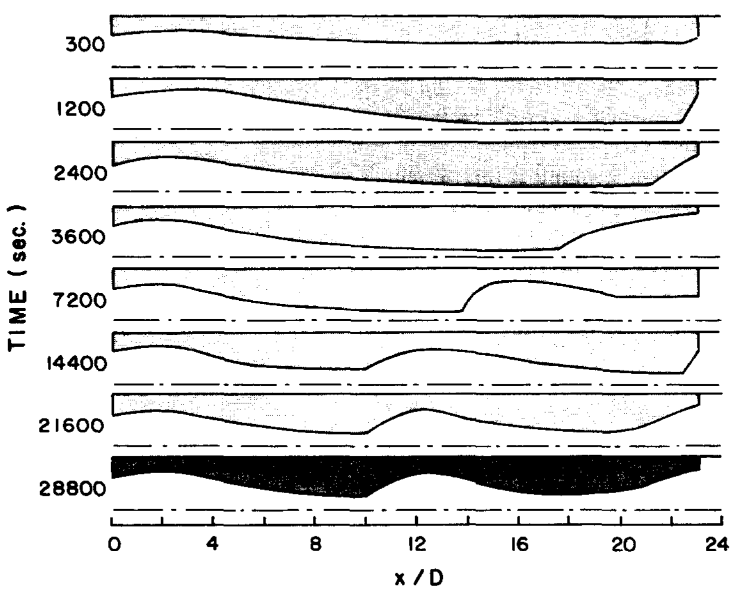

FIG. 4. Instantaneous solid profiles: $d/D = 0.340$, $Re_d = 3440$, $\theta = 5.4$.

maximum value at the reattachment point. Beyond this, the heat transfer coefficient decreases in the redevelopment region. Therefore, the diverging portion corresponds to the separated region and the converging portion corresponds to the redeveloping region. The point where the minimum solid thickness occurs is the reattachment location, which occurs at about 1.3 diameters (7.3 step heights) downstream of the expansion. This is a common value for flows past abrupt expansions [26].

Inspection of Fig. 4 reveals, for $d/D = 0.340$, the same diverging/converging behavior near the test section inlet, with the reattachment point being located at 2.5 diameters (7.6 step heights) downstream of the expansion. At steady state, the upstream expansion point is shifted 4.5 and 6.3 diameters downstream of those for $d/D = 0.643$ and 1.0, respectively, while the upstream expansion point is shifted downstream of those for $d/D = 0.643$ and 1.0 by 4.8 and 5.9 diameters, respectively. This means that the 'ice-band' spacing is within 2.8 and 3.5%, respectively, of those for $d/D = 0.643$ and 1.0, which is within the experimental error. The spacing is within 4% of that predicted by ref. [21]. It should be pointed out that the second expansion point for $d/D = 0.340$ was taken to be the point at which the abrupt expansion occurred. This occurs at 21.4 diameters at 6 h (21 000 s) and 8 h (28 800 s).

Figure 5 was prepared to examine the effect of d/D on the steady-state solid profiles for the same system flow rate (i.e. $Re_D \approx 3400$). The resulting inlet Reynolds numbers are: $Re_d = 3320$, 5320, and 10 200 for $d/D = 1.0$, 0.643, and 0.340, respectively. It is seen that steady-state profiles for $d/D = 0.643$ and 0.340 have the same diverging/converging shapes near the inlet as they did in Figs. 3 and 4. Moreover, the upstream expansion point is displaced by 6.4 and 8.8 diameters for $d/D = 0.643$ and 0.340, respectively, downstream of that for $d/D = 1.0$. As for the 'ice-band' spacing, decreasing d/D from 1.0 to 0.643 reduced the spacing by 6%, while changing d/D from 1.0 to 0.340 reduced the spacing by 11%. When compared to the results of ref. [21] for $d/D = 1.0$, the spacings for $d/D = 0.643$ and 0.340 are within 1 and 5%, respectively.

The effect of the inlet Reynolds number for a given d/D can be examined by comparing the profiles in Fig. 5 to the corresponding steady-state profiles in Figs. 3 and 4. For $d/D = 0.643$, the increase in the inlet Reynolds number shifted the upstream and downstream expansion points downstream by 4.6 diameters. Thus, the ice-band spacing remained unchanged. For $d/D = 0.340$, the upstream and downstream expansion points are shifted downstream of those at the lower Re_d in Fig. 4 by 2.6 and 1.7 tube diameters, respectively. Consequently, the 'ice-band' spacing decreased by about 8%.

Steady-state solid profiles were also obtained for $\theta = 7.7$, 11, and 13 for $d/D = 1.0$, 0.643, and 0.340, respectively, for $Re_D \approx 3400$. For each d/D value, the increase in θ resulted in a decrease in the 'ice-band' spacing and an increase in the number of cycles of expansion and contraction. This is in accordance with the findings of refs. [20, 21]. Similar to the findings for $\theta = 5.4$, the effect of the expansion was confined to the entrance region of the test section and acted to shift the 'ice-band' structure downstream of the no-expansion case. The 'ice-band' spacing for $d/D = 1.0$ ($\theta = 7.5$), 0.643 ($\theta = 11$), and 0.340 ($\theta = 13$) was predicted to within 2.5, 6.1, and 1.7%, respectively, using the correlation of ref. [21].

The preceding discussion of the solid profiles revealed that the expansion was primarily responsible for a downstream shift in the 'ice-band' structure but had essentially no effect on the steady-state 'ice-band' spacing. This is in keeping with the fact that the 'ice-band' spacing tends to be a function of the freezing parameter, θ, only. Moreover, it was found that the 'ice-band' spacing could be predicted to within 8% using the correlation developed for water by ref. [21]. This shows that the correlation of ref. [21] can be successfully applied to paraffin flows and suggests that the correlation is a general one which can be applied to the freezing of liquids other than water and to freezing flows downstream of expansions. It should be mentioned that the 'ice-band' spacing can be used to calculate the number of 'ice-bands' in a given length of pipe, and refs. [20, 21] have shown that the pressure drop is sensitive to the number of 'ice-bands'.

PRESSURE BEHAVIOR

As pointed out earlier, the pressure measurements were performed at the calming section. Therefore, the pressure measured by the gage is the pressure drop

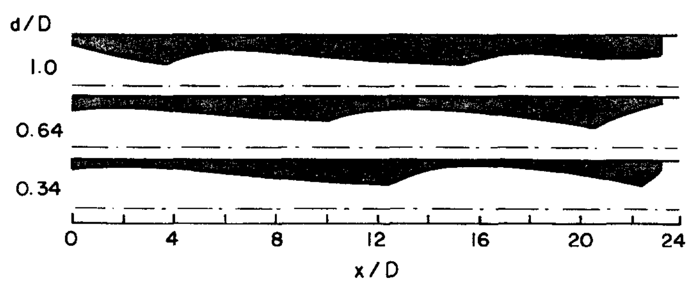

FIG. 5. Effect of d/D on the steady-state solid profile, $Re_D \approx 3400$, $\theta = 5.4$.

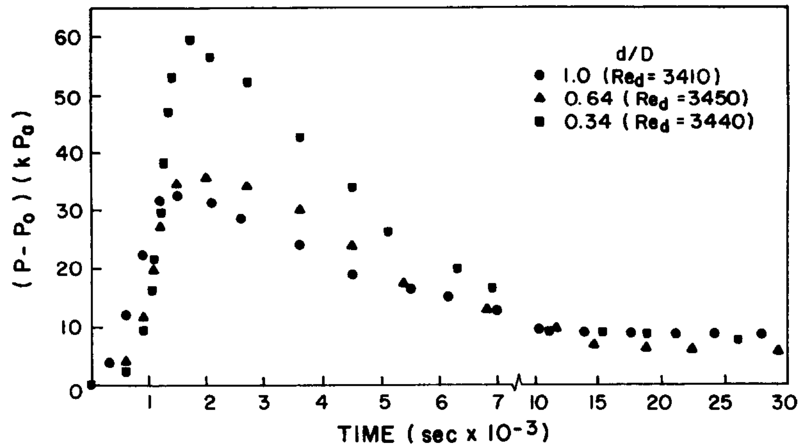

FIG. 6. Effect of d/D on the instantaneous pressure behavior at a fixed inlet Reynolds number for $\theta = 5.4$.

between the gage and the flow loop outlet. Figures 6 and 7 display the instantaneous pressure behavior, plotted as the difference between the instantaneous pressure, P, and the initial pressure before freezing, P_0. The uncertainty in $(P-P_0)$ is $\pm 5\%$, while the uncertainty in the time is ± 2 s.

Figure 6 compares the instantaneous pressure behavior for the three d/D values at the same inlet Reynolds number. It is observed that the pressures initially increase quite rapidly with time until they reach a peak value, after which they decay with time to a steady state. Thomason and Mulligan [23] observed similar behavior for $d/D = 1.0$, $Re_d = 5012$, $\theta = 1.3$, and a coolant side convective heat transfer coefficient five times larger than that in the present investigation. However, the decay terminated in damped pressure oscillations, eventually leading to steady state. No oscillations were observed in the present investigation. However, the peak-to-peak amplitude witnessed by ref. [23] was of the order of the resolution of the pressure gage used in this investigation. Consequently, oscillations may have existed but were not detected.

Figure 6 shows that the peak values lie between 1500 and 2000 s, with the peak value for $d/D = 0.340$ lying well above those for $d/D = 0.643$ and 1.0. A return to the solid profiles in Figs. 2–4 reveals that the initial transient leading to the peak value corresponds to the growth of the uniform tapered layers in the respective figures, with the peak value occurring just after the time where the expansion point starts to move upstream. Note that the expansion point started to migrate between 600 and 1200 s.

After peaking, the pressures drop off until about 10 000 s. Figures 2–4 show that it is during this time period that the most significant upstream movement of the first expansion point occurs. Note, too, that during this time period, the flow passages for the three cases become much less restricted owing to the melting downstream of the expansion point. Consequently, the pressure decreases.

Regarding the dominant peak for $d/D = 0.340$, a comparison of the solid profiles in Figs. 2–4 for times close to that of the peak value clearly shows that the flow passage is more restricted for $d/D = 0.340$. This is primarily due to the fact that the flow rate is about 34 and 52% of those for $d/D = 1.0$ and 0.643, respectively. Also, the fact that the flow rate for $d/D = 0.643$ is about 64% of that for $d/D = 1.0$ is responsible for the differences between these two cases for times

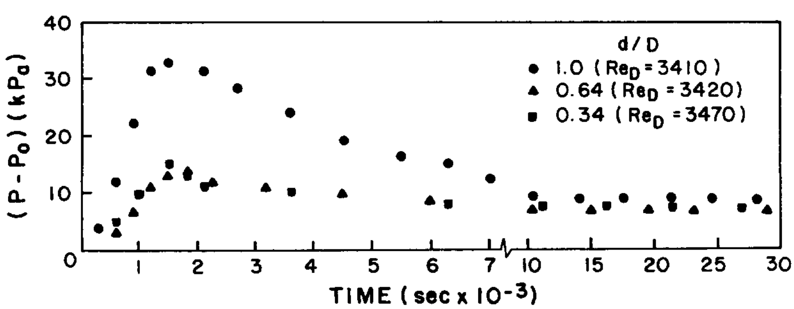

FIG. 7. Effect of d/D on the instantaneous pressure behavior at a fixed test-section Reynolds number for $\theta = 5.4$.

around 2000 s. Note that Fig. 3, for $d/D = 0.643$, shows a more restricted flow passage than that for the same time (2400 s) in Fig. 2 ($d/D = 1.0$).

With regard to the steady-state pressure differences, they appear quite close together. However, if these differences are normalized by $(1/2)\rho V^2(L/D)$, the dimensionless pressure differences are 1.5, 2.8, and 12 for $d/D = 1.0$, 0.643, and 0.340, respectively.

Figure 7 was prepared to examine the effect of d/D on the instantaneous pressure at the same flow rate. It is seen that the instantaneous pressure behavior for $d/D = 0.643$ and 0.340 is about the same, with an initial increase to a maximum value (between 1500 and 2000 s) and a subsequent decay to steady state.

The fact that the decrease in d/D has virtually no effect on the pressure behavior is because the pressure behavior is in response to an average effect, and the effect of d/D is confined to about the first 8 tube diameters. Therefore, the local effect is averaged out. Note that the solid profiles in Figs. 3 and 4 have the same shape after the first 8 diameters. Krall and Sparrow [25] found that the effect of d/D on the local Nusselt number was confined to the first 6–8 pipe diameters.

For $d/D = 1.0$, the pressure curve has the same shape as those for the other d/D values. However, the pressure increases at a much greater rate, and the peak value is about 110% higher, suggesting that the presence of the expansion retards the growth rate of the solid during the early development of the solid layer. This can be attributed to the turbulence generated by the passage of the flow through the inlet expansion.

At steady state, the pressures for $d/D = 0.643$ and 0.340 are within the experimental uncertainty ($\pm 5\%$) of each other, while the pressures for $d/D = 1.0$ lie about 20% above those for the other diameter ratios. Note that the scale of the graph masks this difference. Figure 5 shows that the solid layer is thicker for $d/D = 1.0$, which is the reason for the increased pressure. Thus, the expansion acts to retard freezing.

The fact that the difference between the results for $d/D = 1.0$ and the other diameter ratios decreases markedly with time can be attributed to the development of the 'ice-band' structure. Note Figs. 2–4 show that, as time passes, the shapes of the respective flow passages are quite similar. This is responsible for the considerably smaller differences in pressure between the expansion and no-expansion cases at steady state.

FREEZE-OFF

The objective here was to examine the effect of d/D on the θ value at which freeze-off occurs. All of the freeze-off experiments were performed at the highest flow rate (i.e. $Re_D \approx 3400$). The basic procedure consisted of performing a series of data runs for each diameter ratio at successively higher θ values until freeze-off occurred.

Figures 8–10 exhibit the timewise pressure behavior leading to freeze-off for $d/D = 1.0$, 0.643, and 0.340, respectively. Pressure plots for θ values which resulted in the pressure going to a steady-state value are also included. The θ values for freeze-off and steady state are as close as could be attained to the critical value at which freeze-off occurs.

In a manner similar to that observed by ref. [23], the respective figures show that when freeze-off occurs, the pressure goes through a smooth rapid transient, with total tube blockage occurring within 20 min (1200 s) for all of the cases considered. It should be mentioned that at the end of the transient, the pressure reading instantaneously jumped to the pressure setting of the pressure relief valve used to protect the system. This was twice the value exhibited on the plot. The instantaneous jump indicated complete tube blockage, which was verified by visual inspection.

Figure 8 shows, for $d/D = 1.0$, that freeze-off occurs for $7.5 < \theta \leqslant 8.5$. The pressure characteristic for $\theta = 7.5$ exhibits the same behavior that was observed for $\theta = 5.4$, i.e. an increase followed by a decrease, which terminates at a steady-state value. The decrease was linked to the upstream migration of the expansion point near the exit which resulted in melting due to the increased turbulence caused by the flow moving past the expansion point. On the other hand, for $\theta = 8.5$, the pressure increases until freeze-off is achieved, indicating insufficient time for the expansion point to move upstream to the point where the additional turbulence can cause enough melting to retard the growth of the solid. Figure 2 shows that the solid stops growing after about 1200 s. Indeed, an examination of the frozen-off solid revealed a smoothly tapered flow passage, which terminated at the expansion point near the exit (i.e. at 22 diameters).

Reference [21] also found that freeze-off initially occurred at the expansion points. However, several frozen-off expansion points (i.e. location of minimum diameter) were observed to occur over the length of the duct, with liquid being trapped in the pockets separating these locations. Essentially, ref. [21] observed a highly developed 'ice-band' structure which had frozen off at the expansion points. The difference between the results of the present study and those of ref. [21] is probably due to the fact that the θ value in ref. [21] is higher, resulting in more expansion points and a smaller 'ice-band' spacing [20, 21].

Figure 9 shows that the presence of the expansion ($d/D = 0.643$) postpones freeze-off until $11 < \theta \leqslant 13$. Note that a steady state was achieved for $\theta = 11$, while freeze-off occurred at $\theta = 8.5$ for $d/D = 1.0$. It was pointed out earlier that the turbulence resulting from the flow separation at the inlet acts to retard the initial growth rate of the solid and hence the growth rate of the pressure characteristic. Then, as time passes, the flow passages become quite similar for $d/D = 1.0$ and 0.643 (see Figs. 2 and 3), owing to the upstream

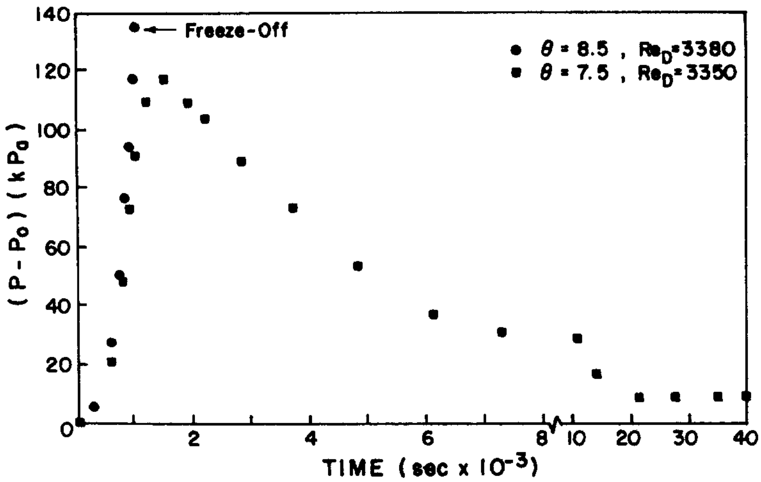

FIG. 8. Instantaneous pressure behavior for freeze-off and near freeze-off conditions, d/D = 1.0.

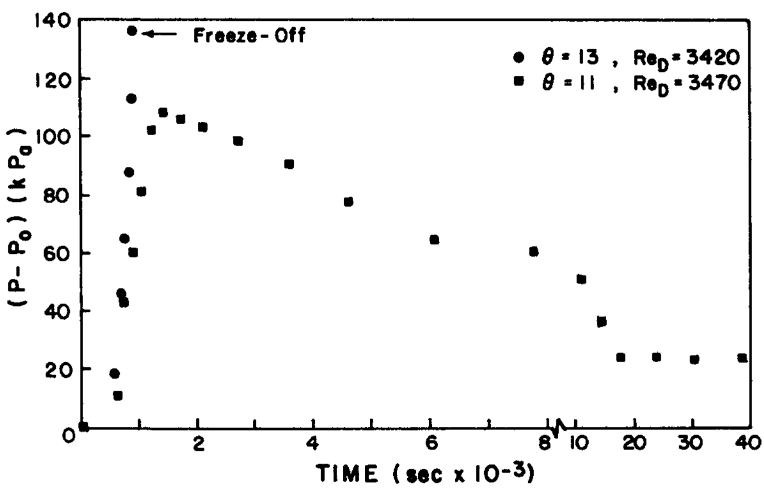

FIG. 9. Instantaneous pressure behavior for freeze-off and near freeze-off conditions, d/D = 0.643.

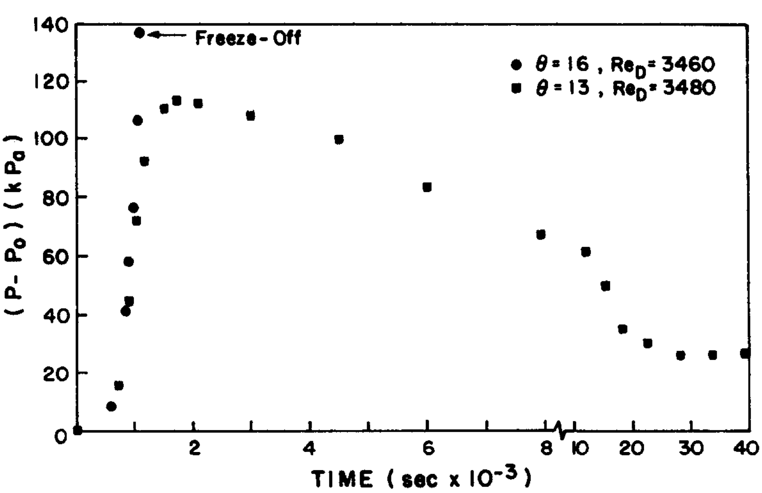

FIG. 10. Instantaneous pressure behavior for freeze-off and near freeze-off conditions, d/D = 0.340.

migration of the expansion point and the subsequent development of the 'ice-band' structure.

For this case ($d/D = 0.643$), it is believed that the effect of the turbulence caused by the flow through the inlet expansion postpones freeze-off long enough for the expansion point to move upstream to a point at which the growth rate of the solid is arrested, causing the pressure to peak out. Then, as observed for $\theta = 5.4$, the solid layer actually diminishes slightly with the further upstream movement of the expansion point causing the pressure to drop until a steady-state value is reached.

It should be pointed out that the steady-state pressure difference for this case ($d/D = 0.643$) is about 2.4 times greater than that for $d/D = 1.0$, indicating a larger degree of flow blockage. Examination of the solid confirmed this. In addition, there were more cycles of expansion and contraction resulting from the increase in θ. It was shown in refs. [20, 21] that the pressure drop increases with the number of cycles.

Figure 10 displays the pressure results for $d/D = 0.340$. It is seen that freeze-off now occurs for $13 < \theta \leqslant 16$. It is also observed that freeze-off does not occur for $\theta = 13$ as it did for $d/D = 0.643$. Rather, a steady state is achieved for $\theta = 13$. At steady state, the pressure difference is about 20% greater than that for $d/D = 0.643$ and about 2.9 times greater than that for $d/D = 1.0$. These differences are due to increased flow blockage and an increased number of expansions and contractions due to the increased θ value.

It should be mentioned that the effect of changing d/D from 0.643 to 0.340 on freeze-off may be less than indicated here. Recall that the pressure behavior for these two cases at $\theta = 5.4$ was nearly the same. This was attributed to the fact that the effect of changing the diameter ratio is rather a local effect. Attempts were made to see if freeze-off occurred at θ values below 16, but for θ values in this range, the θ value could not be preset so it would lie between 13 and 16.

An examination of the frozen-off solids revealed again that freeze-off first occurs at the expansion point which occurs near the exit. Freeze-off occurred when the expansion point was at $x/D = 21$ ($\theta = 13$) and 19 ($\theta = 16$) for $d/D = 0.643$ and 0.340, respectively. Again, the ice-band structure was in its early stages of development when freeze-off occurred, which is in agreement with the pressure transient.

CONCLUDING REMARKS

An experimental investigation was undertaken to examine the effect of an abrupt channel expansion on the freezing of a paraffin flow downstream of the expansion. Results were obtained for expansion ratios, d/D, of 1.0 (no expansion), 0.643, and 0.340 at a fixed system flow rate ($Re_D \approx 3400$) and a fixed inlet Reynolds number, $Re_d \approx 3400$ (i.e. the flow rate was varied to give a fixed Re_d).

Instantaneous and steady-state profile results revealed the existence of a classical 'ice-band' structure for all of the parameter values considered. It was found that the steady-state 'ice-band' spacing was a function of the freezing parameter (θ) only and could be predicted to within 8% using the correlation of ref. [21], developed for a water flow in a constant-area duct. The latter finding suggests that the 'ice-band' spacing is independent of the fluid properties and inlet geometry. However, additional studies involving other liquids should be undertaken to confirm this observation.

It was also found that the presence of the expansion acts to retard the growth rate of the solid during early times and thus causes freeze-off to occur at higher θ values. Freeze-off occurred for $7.5 < \theta \leqslant 8.5$, $11 < \theta \leqslant 13$, and $13 < \theta \leqslant 16$ for $d/D = 1.0$, 0.643, and 0.340, respectively.

Acknowledgement—This work was supported by the Louisiana State University Center for Energy Studies under Grant No. 82-02-16.

REFERENCES

1. K. Stefan, Influence of heat transfer on melting and solidification in forced flow, *Int. J. Heat Mass Transfer* **12,** 199–214 (1967).
2. M. N. Özisik and J. C. Mulligan, Transient freezing of liquids in forced flow inside circular tubes, *J. Heat Transfer* **91,** 385–389 (1969).
3. C. Cho and M. N. Özisik, Transient freezing of liquids in turbulent flow inside tubes, *J. Heat Transfer* **101,** 465–468 (1979).
4. A. A. Shibani and M. N. Özisik, A solution of freezing of liquids of low Prandtl number in turbulent flow between parallel plates, *J. Heat Transfer* **99,** 20–24 (1977).
5. J. L. Sproston, Two-dimensional solidification in pipes of rectangular section, *Int. J. Heat Mass Transfer* **99,** 1493–1501 (1981).
6. G. S. H. Lock and R. H. Nyren, Analysis of fully-developed ice formation in a convectively-cooled circular tube, *Int. J. Heat Mass Transfer* **14,** 825–834 (1971).
7. K. C. Cheng and S. L. Wong, Liquid solidification in a convectively-cooled parallel-plate channel, *Can. J. Chem. Engng* **55,** 149–155 (1977).
8. K. C. Cheng and S. L. Wong, Asymmetric solidification of flowing liquid in a convectively-cooled parallel plate channel, *Appl. Scient. Res.* **33,** 309–335 (1977).
9. M. S. Sadeghipour, M. N. Özisik and J. C. Mulligan, The effect of external convection on freezing in steady turbulent flow in a tube, *Int. J. Engng Sci.* **22,** 135–148 (1984).
10. R. D. Zerkle and J. E. Sunderland, The effect of liquid solidification in a tube upon laminar-flow heat transfer and pressure drop, *J. Heat Transfer* **90,** 183–190 (1968).
11. C. A. Depew and R. C. Zenter, Laminar flow heat transfer and pressure drop with freezing at the wall, *Int. J. Heat Mass Transfer* **12,** 1710–1714 (1969).
12. J. C. Mulligan and D. D. Jones, Experiments on heat transfer and pressure drop in a horizontal tube with internal solidification, *Int. J. Heat Mass Transfer* **19,** 213–219 (1976).
13. R. R. Gilpin, The morphology of the ice structure in a pipe at or near transition Reynolds numbers, *A.I.Ch.E. Symp. Ser.* **75,** 89–94 (1979).
14. G. J. Hwang and J. P. Sheu, Liquid solidification in the combined hydrodynamic and thermal entrance region of a circular tube, *Can. J. Chem. Engng* **54,** 66–71 (1976).
15. S. B. Thomason, J. C. Mulligan and J. Everhart, The

effect of internal solidification on turbulent flow heat transfer and pressure drop in a horizontal tube, *J. Heat Transfer* **100**, 387–394 (1978).
16. N. DesRuisseaux and R. D. Zerkle, Freezing of hydraulic systems, *Can. J. Chem. Engng* **47**, 233–237 (1969).
17. P. Sampson and R. D. Gibson, A mathematical model of nozzle blockage by freezing, *Int. J. Heat Mass Transfer* **24**, 231–241 (1981).
18. E. P. Martinez and R. T. Beaubouf, Transient freezing in laminar tube flow, *Can. J. Chem. Engng* **50**, 445–449 (1972).
19. T. Hirata, Effects of friction losses in water-flow pipe systems on freeze-off conditions, *Int. J. Heat Mass Transfer* **29**, 949–951 (1986).
20. R. R. Gilpin, Ice formation in a pipe containing flows in the transition and turbulent regimes, *J. Heat Transfer* **103**, 363–368 (1981).
21. T. Hirata and M. Ishihara, Freeze-off conditions of a pipe containing a flow of water, *Int. J. Heat Mass Transfer* **28**, 331–337 (1985).
22. N. Seki, S. Fukusako and G. W. Younan, Ice-formation phenomena for water flow between two cooled parallel plates, *J. Heat Transfer* **106**, 498–505 (1984).
23. S. B. Thomason and J. C. Mulligan, Experimental observations of flow instability during turbulent freezing in a horizontal tube, *J. Heat Transfer* **102**, 782–784 (1980).
24. E. M. Sparrow, G. A. Gurtcheff and T. A. Myrum, Correlation of melting results for both pure substances and impure substances, *J. Heat Transfer* **108**, 649–653 (1986).
25. K. M. Krall and E. M. Sparrow, Turbulent heat transfer in the separated, reattached, and redevelopment regions of a circular tube, *J. Heat Transfer* **88**, 131–136 (1961).
26. J. W. Baughn, M. A. Hoffman, R. K. Takahashi and B. E. Launder, Local heat transfer downstream of an abrupt expansion in a circular channel with constant heat flux, *J. Heat Transfer* **106**, 789–796 (1984).

GEL D'UN ECOULEMENT DE PARAFFINE EN AVAL D'UN ELARGISSEMENT BRUSQUE

Résumé—On étudie expérimentalement le gel d'un écoulement de paraffine en aval d'un élargissement brusque. Des résultats obtenus pour trois rapports d'élargissement (d/D) à débit constant ($Re_D \approx 3400$) et avec un nombre de Reynolds d'entrée constant ($Re_d \approx 3400$) montrent que l'espacement de la "bande de glace" est une fonction du seul paramètre de gel (θ) et peut être prédit à mieux que 8% en utilisant une formule développée pour l'écoulement d'eau dans un canal à section constante. Les résultats montrent aussi que l'effet de l'élargissement est de causer un dégel à des valeurs plus élevées de θ avec des valeurs $7{,}5 < \theta \leqslant 8{,}5$, $11 < \theta \leqslant 13$ et $13 < \theta \leqslant 16$ respectivement pour $d/D = 1{,}0$ (pas d'élargissement), 0,643 et 0,340.

ERSTARRUNG EINER PARAFFINSTRÖMUNG HINTER EINER STUFENFÖRMIGEN QUERSCHNITTSERWEITERUNG

Zusammenfassung—Das Erstarrungsverhalten einer Paraffinströmung hinter einer stufenförmigen Querschnittserweiterung wird experimentell untersucht. Die Ergebnisse für 3 unterschiedliche Verhältnisse der Querschnittserweiterung (d/D) bei konstantem System-Massenstrom ($Re_D \approx 3400$) und konstanter Reynolds-Zahl am Eintritt ($Re_d \approx 3400$) zeigen, daß die Ausdehnung der Erstarrungszone vom Erstarrungsparameter (θ) abhängt und mit einer Genauigkeit von 8% vorherberechnet werden kann. Die hierzu verwendete Korrelation wurde für Wasser in einem Strömungskanal mit konstantem Querschnitt entwickelt. Die Ergebnisse zeigen auch, daß die Querschnittserweiterung ein Abtauen bei höheren θ-Werten bewirkt. Das Abtauen tritt für $d/D = 1{,}0$ (keine Erweiterung) bei $7{,}5 < \theta \leqslant 8{,}5$ auf, für $d/D = 0{,}643$ bei $11 < \theta \leqslant 13$ und für $d/D = 0{,}340$ bei $13 < \theta \leqslant 16$.

ЗАТВЕРДЕВАНИЕ ПОТОКА ПАРАФИНА ЗА ВНЕЗАПНЫМ РАСШИРЕНИЕМ

Аннотация—Экспериментально исследуется затвердевание потока парафина за внезапным расширением. Результаты для трех различных степеней расширения канала (d/D) при постоянных расходе ($Re_D \approx 3400$) и числе Рейнольдса на входе ($Re_d \approx 3400$) показывают, что расстояние между отдельными "затвердевшими полосами" зависит только от параметра затвердевания θ и может определяться с точностью до 8% по соотношению, полученному для течения воды в канале с постоянным проходным сечением. Результаты также свидетельствуют о том, что за счет эффекта расширения затвердевание происходит при более высоких значениях θ, а именно, в интервалах $7{,}5 < \theta \leqslant 8{,}5$; $11 < \theta \leqslant 13$ и $13 < \theta \leqslant 16$ при отношениях $d/D = 1{,}0$ (без расширения); 0,643 и 0,340.